

A CASPT2 Study of the Electronic Spectrum of Hexacyanoosmate(III)

Willem Van den Heuvel,* Marc F. A. Hendrickx, and Arnout Ceulemans

Department of Chemistry, Katholieke Universiteit Leuven, Celestijnenlaan 200F, B-3001 Leuven, Belgium

Received March 9, 2007

CASPT2 calculations reveal that the ligand field splitting parameter Δ_o of $[\text{Os}(\text{CN})_6]^{3-}$ is much higher than previously proposed values of $\pm 38\,000\text{ cm}^{-1}$. In line with the expected increase down a transition-metal group, Δ_o is found to be $\pm 55\,000\text{ cm}^{-1}$, excluding the possible appearance of ligand field transitions in the UV–vis spectrum. Instead, the calculations confirm that the observed spectrum arises from the three lowest symmetry-allowed ligand-to-metal charge-transfer (LMCT) excitations. Spin–orbit coupling in the ground state is found to be about 4350 cm^{-1} , leading to a spin–orbit coupling constant ζ of $\pm 2900\text{ cm}^{-1}$. Spin–orbit coupling in the ${}^2T_{1u}$ LMCT states is found not to be negligible, contrary to previous belief.

1. Introduction

The experimental electronic spectrum of the octahedral $[\text{Os}(\text{CN})_6]^{3-}$ complex shows three regions of broad absorptions,^{1–3} very similar to the spectra of its Fe^{III} ^{1,4} and Ru^{III} ² analogues. It is now believed that the absorption bands in $[\text{Fe}(\text{CN})_6]^{3-}$ originate from excitations to ungerade ligand-to-metal charge-transfer (LMCT) states. The ground-state t_{2g}^5 configuration leads to a simple LMCT spectrum since a one-electron excitation from a ligand orbital into the t_{2g} shell fills it completely, resulting in a one-to-one correspondence between the excited states and the ligand orbitals. The highest occupied σ and π orbitals of the CN^- ligands give rise to three ungerade orbitals after symmetry adaptation, namely, $t_{1u}\sigma$, $t_{2u}\pi$, and $t_{1u}\pi$, resulting in three symmetry-allowed LMCTs: ${}^2T_{2g} \rightarrow {}^2T_{1u} a$, ${}^2T_{2g} \rightarrow {}^2T_{2u}$, and ${}^2T_{2g} \rightarrow {}^2T_{1u} b$, respectively. Although some peaks flanking these three absorptions in $[\text{Fe}(\text{CN})_6]^{3-}$ were first assigned to ligand field (d–d) transitions,¹ later work suggested that these are instead vibrational components of the LMCT transitions.⁴ Evidence for this is found in three observations. First, the splitting between those peaks is about 2100 cm^{-1} , in accordance with the CN^- stretching frequency. Second, the signs of the bands, including the presumed vibrational progression, in magnetic circular dichroism (MCD) spectroscopy are in agreement

with those expected for ${}^2T_{2g} \rightarrow {}^2T_{1u}$ and ${}^2T_{2g} \rightarrow {}^2T_{2u}$ transitions. And third, the striking resemblance between the spectra of the Fe^{III} , Ru^{III} , and Os^{III} complexes² leads to the conclusion that the presence of d–d transitions is very unlikely. It is indeed well-known that the ligand field parameter Δ_o increases by 25–50% when the central metal ion is replaced by its next-row congener,⁵ so that d–d absorptions should blue-shift through the spectrum. Although the previous assignment of d–d transitions in the $[\text{Fe}(\text{CN})_6]^{3-}$ spectrum is now believed to be wrong, it has been confirmed by CASPT2 calculations⁶ that these transitions do occur in the same energy region, so the previously proposed Δ_o value of about $35\,000\text{ cm}^{-1}$ is quite correct after all. An example of such an increase of Δ_o is provided by the hexacyanides of the d^6 ions of Co^{III} and its fourth-row congener Rh^{III} : Δ_o increases from $32\,200\text{ cm}^{-1}$ in $[\text{Co}(\text{CN})_6]^{3-}$ to $45\,500\text{ cm}^{-1}$ in $[\text{Rh}(\text{CN})_6]^{3-}$.⁵

Focusing now on $[\text{Os}(\text{CN})_6]^{3-}$, based on a 25% increase per row, we would expect Δ_o to be about $55\,000\text{ cm}^{-1}$. However, in the first spectroscopic study of this complex,¹ a value of only $38\,000\text{ cm}^{-1}$ was proposed, based on an assignment of two bands in the spectrum. Even very recently, a similar value of $38\,500\text{ cm}^{-1}$ was used to fit magnetic data.³ In a MCD study of $[\text{Ru}(\text{CN})_6]^{3-}$ and $[\text{Os}(\text{CN})_6]^{3-}$, the authors arrived at the conclusion that the main features of the spectra arise from the three ungerade LMCTs and their vibronic progression, following arguments similar to those mentioned

* To whom correspondence should be addressed. E-mail: willem.vandenheuvel@chem.kuleuven.be.

- (1) Alexander, J. J.; Gray, H. B. *J. Am. Chem. Soc.* **1968**, *90*, 4260.
- (2) Kang, H. W.; Moran, G.; Krausz, E. *Inorg. Chim. Acta* **1996**, *249*, 231.
- (3) Albores, P.; Slep, L. D.; Baraldo, L. M.; Baggio, R.; Garland, M. T.; Rentschler, E. *Inorg. Chem.* **2006**, *45*, 2361.
- (4) Gale, R.; McCaffery, A. J. *J. Chem. Soc., Dalton Trans.* **1973**, 1344.

(5) Lever, A. B. P. *Inorganic Electronic Spectroscopy*; Elsevier Publishing Company: Amsterdam, 1968.

(6) Pierloot, K.; Van Praet, E.; Vanquickenborne, L. G. *J. Phys. Chem.* **1993**, *97*, 12220.

above.² With this contribution, we want to support this conclusion with ab initio CASPT2 calculations on the ligand field and charge-transfer spectrum of $[\text{Os}(\text{CN})_6]^{3-}$. In particular, it will be shown that Δ_o is indeed much higher than the previously proposed values. The CASPT2 method has proven its value in inorganic electronic spectroscopy calculations,⁷ including calculations on transition-metal cyanides.^{6,8–11} Recently, time-dependent density functional theory has also been applied to transition-metal carbonyls and cyanides.^{12–14}

2. Computational Details

Single-point calculations were performed on the octahedral $[\text{Os}(\text{CN})_6]^{3-}$ complex, using averaged experimental bond distances (the X-ray structure shows only minor deviations from octahedral (O_h) symmetry):³ 2.06 Å for the Os–C bond and 1.15 Å for the C–N bond. The transition energies were obtained as the difference between the total electronic energies of the excited states and the ground state. The energies themselves were calculated by a second-order perturbational approach (CASPT2)^{15,16} based on a multiconfigurational reference wave function (CASSCF).¹⁷ All calculations were performed with the *MOLCAS* 6.2 software.¹⁸

For calculations not involving spin–orbit coupling, we chose a relativistic ECP (effective core potential) basis set (Cowan-Griffin relativistic core AIMP)¹⁹ on Os in combination with an ANO-S basis²⁰ on the C and N atoms, as available in *MOLCAS*. The ECP on Os replaces the $[\text{Kr}]4d^{10}4f^{14}5s^2$ electron core. The valence of Os is described by a $(13s10p9d5f)/[3s3p4d2f]$ basis set. The ANO-S basis on C and N is contracted as follows: $(10s6p3d)/[3s2p1d]$. The use of symmetry in *MOLCAS* is restricted to point groups without degenerate irreducible representations. Therefore, we used the D_{2h} subgroup of O_h that places the CN^- ligands on the twofold axes. Furthermore, the mixing of orbitals belonging to different O_h irreducible representations was prevented.

The central step in a CASSCF calculation is the construction of the active space. For ligand field states, an active space of 9 electrons in 10 orbitals (9 in 10) has been proven sufficient to include the most important static correlation effects in first-row transition-metal cyanide complexes.⁶ It consists of the bonding/antibonding pair e_g/e_g^* , whose orbitals show a substantial cova-

lency between ligand and d orbitals, and the metal t_{2g} –d shell together with its “double shell”. After the first calculations, it was clear that the conditions leading to the choice of this active space were also fulfilled in our third-row complex, although static correlation and the double-shell effect were smaller, as expected for the heavier transition-metal compounds.²¹ We shall refer to this (9 in 10) space as AS1. For the charge-transfer states, AS1 obviously has to be extended with the appropriate ligand orbitals, while keeping the computational limitations on the size of the active space in mind. Unless otherwise specified, the CASSCF wave functions and energies were obtained as single roots. In the CASPT2 step, the following electrons were correlated: 5p, 5d of Os and 2s, and 2p of C and N. A small CASPT2 level shift of 0.05 E_h was applied to prevent “intruder states”.²²

In *MOLCAS*, spin–orbit coupling (SOC) is introduced by diagonalizing the SOC matrix between a set of CASSCF functions, using the CASPT2 energies as SOC-free energies (RASSI-SO method^{23,24}). The method is based on the partitioning of the Douglas–Kroll Hamiltonian in a scalar relativistic part and a spin–orbit coupling part.²⁴ The scalar part is already included in the CASSCF step while the SOC part is diagonalized in the SOC step. For these calculations, we used all-electron ANO-RCC basis sets,²⁵ which are constructed to include scalar relativistic effects, using the Douglas–Kroll Hamiltonian. The following contractions were used: $(24s21p15d11f4g)/[8s7p5d3f2g]$ on Os and $(14s9p4d3f2g)/[3s2p1d]$ on C and N. This basis set also allowed the correlation of the Os 5s electrons in the CASPT2 step. The CASSCF functions used in the SOC calculation have to be calculated within the same active space. This confronts us with a rather difficult situation and forces us to treat the SOC in an approximate way, as will be discussed in the text. Some idea of the accuracy of the computational model used may be obtained by noticing that a CASPT2 optimization (using the ECP basis) of the Os–C distance agrees with the experimental distance. By calculating the ground-state energy with CASPT2 and AS1 for a few Os–C distances around the minimum—keeping the C–N distance at 1.15 Å—the minimum of a fitted cubic polynomial was found at 2.06 Å. All SOC-free transition energies were calculated with the ECP basis set, while those including SOC were calculated with the all-electron ANO-RCC basis set, unless specified otherwise.

3. Results and Discussion

Since we are interested in the value of Δ_o and consequently the possibility of ligand field transitions in the experimental spectrum of $[\text{Os}(\text{CN})_6]^{3-}$, we considered the lowest part of the ligand field spectrum without SOC. Energies of transition from the ${}^2T_{2g}$ ground state to all the states related to the formal $t_{2g}^4 e_g^1$ configuration as well as to the high-spin ${}^6A_{1g}$ ($t_{2g}^3 e_g^2$) state were calculated. The results are listed in Table 1. It is immediately clear that the complex resides in a very strong ligand field: the high-spin-state ${}^6A_{1g}$, which requires two electrons bridging the ligand field gap, appears far above

- (7) Pierloot, K. *Mol. Phys.* **2003**, *101*, 2038.
- (8) Hendrickx, M. F. A.; Mironov, V. S.; Chibotaru, L. F.; Ceulemans, A. *J. Am. Chem. Soc.* **2003**, *125*, 3694.
- (9) Hendrickx, M. F. A.; Chibotaru, L. F.; Ceulemans, A. *Inorg. Chem.* **2003**, *42*, 590.
- (10) Hendrickx, M. F. A.; Mironov, V. S.; Chibotaru, L. F.; Ceulemans, A. *Inorg. Chem.* **2004**, *43*, 3142.
- (11) Clima, S.; Hendrickx, M. F. A. *Chem. Phys. Lett.* **2005**, *411*, 121.
- (12) Hummel, P.; Oxgaard, J.; Goddard, W. A., III; Gray, H. B. *Inorg. Chem.* **2005**, *44*, 2454.
- (13) Hummel, P.; Halpern-Manners, N. W.; Gray, H. B. *Inorg. Chem.* **2006**, *45*, 7397.
- (14) Hummel, P.; Winkler, J. R.; Gray, H. B. *Theor. Chem. Acc.* DOI: 10.1007/s00214-006-0236-8. Published Online: Jan 12, 2007.
- (15) Andersson, K.; Malmqvist, P.-Å.; Roos, B. O.; Sadlej, A. J.; Wolinski, K. *J. Phys. Chem.* **1990**, *94*, 5483.
- (16) Andersson, K.; Malmqvist, P.-Å.; Roos, B. O. *J. Chem. Phys.* **1992**, *96*, 1218.
- (17) Malmqvist, P.-Å.; Rendell, A.; Roos, B. O. *J. Phys. Chem.* **1990**, *94*, 5477.
- (18) Karlström, G.; Lindh, R.; Malmqvist, P.-Å.; Roos, B. O.; Ryde, U.; Veryazov, V.; Widmark, P.-O.; Cossi, M.; Schimmelpfennig, B.; Neogrady, P.; Seijo, L. *Comput. Mater. Sci.* **2003**, *28*, 222.
- (19) Casarrubios, M.; Seijo, L. *J. Chem. Phys.* **1999**, *110*, 784.
- (20) Pierloot, K.; Dumez, B.; Widmark, P.-O.; Roos, B. O. *Theor. Chim. Acta* **1995**, *90*, 87.

- (21) Pierloot, K. In *Computational Organometallic Chemistry*; Cundari, T. R., Ed.; Marcel Dekker, Inc.: New York, 2001.
- (22) Roos, B. O.; Andersson, K.; Fülischer, M. P.; Serrano-Andrés, L.; Pierloot, K.; Merchán, M.; Molina, V. *J. Mol. Struct. (THEOCHEM)* **1996**, *388*, 257.
- (23) Malmqvist, P.-Å.; Roos, B. O.; Schimmelpfennig, B. *Chem. Phys. Lett.* **2002**, *357*, 230.
- (24) Roos, B. O.; Malmqvist, P.-Å. *Phys. Chem. Chem. Phys.* **2004**, *6*, 2919.
- (25) Roos, B. O.; Lindh, R.; Malmqvist, P.-Å.; Veryazov, V.; Widmark, P. O. *J. Phys. Chem. A* **2005**, *109*, 6575.

Table 1. Ligand Field Excitation Energies ΔE of $[\text{Os}(\text{CN})_6]^{3-}$ Calculated with AS1 and without SOC^a

state D_{2h}	state O_h	main configuration	CASPT2 ($\Delta E/\text{cm}^{-1}$)
${}^2\text{B}_{1g}$	${}^2\text{T}_{2g}$	t_{2g}^5	0
${}^4\text{B}_{1g}$	${}^4\text{T}_{1g}$	$t_{2g}^4 e_g^1$	46 173
${}^4\text{B}_{1g}$	${}^4\text{T}_{2g}$	$t_{2g}^4 e_g^1$	49 125
${}^2\text{B}_{1g}$	${}^2\text{T}_{1g}$ a	$t_{2g}^4 e_g^1$	51 326
${}^2\text{A}_g$	${}^2\text{A}_{2g}$	$t_{2g}^4 e_g^1$	53 268
${}^2\text{B}_{1g}$	${}^2\text{T}_{2g}$ a	$t_{2g}^4 e_g^1$	54 330
${}^2\text{A}_g$	${}^2\text{E}_g$ a	$t_{2g}^4 e_g^1$	54 941
${}^2\text{B}_{1g}$	${}^2\text{T}_{2g}$ b	$t_{2g}^4 e_g^1$	56 139
${}^2\text{B}_{1g}$	${}^2\text{T}_{1g}$ b	$t_{2g}^4 e_g^1$	57 928
${}^2\text{A}_g$	${}^2\text{A}_{1g}$	$t_{2g}^4 e_g^1$	59 172
${}^2\text{A}_g$	${}^2\text{E}_g$ b	$t_{2g}^4 e_g^1$	63 135
${}^6\text{A}_g$	${}^6\text{A}_{1g}$	$t_{2g}^3 e_g^2$	86 990

^a State-averaged CASSCF was used to calculate the pairs ${}^4\text{T}_{1g}/{}^4\text{T}_{2g}$ and ${}^2\text{T}_{2g}$ b/ ${}^2\text{T}_{1g}$ b.

the others. We can obtain estimates for Δ_o and the Racah parameters B and C by fitting these energies to the ligand field energy expressions in the strong field limit.²⁶ We used a least-squares fit and weighted each state according to its total degeneracy. The two ${}^2\text{E}_g$ states were not included because their energy expressions are not linear in B and C . We obtained the following values: $\Delta_o = 54\,809\text{ cm}^{-1}$, $B = 337\text{ cm}^{-1}$, and $C = 1737\text{ cm}^{-1}$.

This high value of Δ_o clearly contrasts with the previously proposed values of about $38\,000\text{ cm}^{-1}$ ^{1,3} but instead agrees well with the value of $55\,000\text{ cm}^{-1}$ estimated by a 25% increase per transition-metal row. In that sense, there is nothing surprising about the ligand field spectrum of $[\text{Os}(\text{CN})_6]^{3-}$. The list of transition energies in Table 1 is, however, not meant to represent an accurate picture of the real position of the ligand field states since spin-orbit coupling was not taken into account. We have not attempted a calculation of the ligand field SOC states for two reasons. First, the SOC in the complex is quite large as testified by the approximate SOC constant $\zeta \approx 2900\text{ cm}^{-1}$ (see below). A reliable SOC calculation would therefore require a large set of spin-free states to interact, including LMCTs and MLCTs, since these fall in the same energy region. Such an amount of states cannot be covered by one and the same active space. Second, as the first excitation in Table 1 only appears at $46\,173\text{ cm}^{-1}$, which is well above the lowest LMCT's (see below), none of the ligand field states can contribute to the recorded UV-vis spectrum, even when SOC is taken into account. A detailed calculation of the SOC effect for the ligand field excited states would therefore not contribute to the clarification of the origin of the absorptions.

For the ${}^2\text{T}_{2g}$ ground state, we do need a sufficient approximation of the SOC splitting in order to explain the

Table 2. LMCT Excitation Energies ΔE of $[\text{Os}(\text{CN})_6]^{3-}$

active space	state D_{2h}	state O_h	state O_h^*	CASPT2 ^a		
				ECP ($\Delta E/\text{cm}^{-1}$)	RCC ($\Delta E/\text{cm}^{-1}$)	SOC ($\Delta E/\text{cm}^{-1}$)
	${}^2\text{B}_{1g}$	${}^2\text{T}_{2g}$	E''_g	0	0	0
AS2	${}^2\text{B}_{1u}$	${}^2\text{T}_{1u}$ a	U'_u	23 620	22 798	24 861
			E'_u			27 145
AS3	${}^2\text{B}_{1u}$	${}^2\text{T}_{2u}$	U'_u	35 239	37 069	39 952
			E''_u			39 981
AS2	${}^2\text{B}_{1u}$	${}^2\text{T}_{1u}$ b	U'_u	37 546	38 225	40 639
			E'_u			42 161

^a The CASPT2 energies of the ${}^2\text{T}_{1u}$ states are the eigenvalues of the SOC-free Hamiltonian matrix within these two states.

spectrum. The fact that the ground state is well-separated from the first gerade excited states makes it reasonable to treat SOC in first order within the ${}^2\text{T}_{2g}$ term. This means diagonalizing the SOC matrix within the CASSCF functions of the ground state. Under the effect of SOC, a ${}^2\text{T}_{2g}$ term reduces to a E''_g and a U'_g term of the double group O_h^* , located at $-\zeta$ and $+(\zeta/2)$, respectively, according to simple ligand field theory.²⁶ The calculated splitting (using AS1) is 4342 cm^{-1} , leading to a SOC parameter ζ of 2895 cm^{-1} . This result supports the assignment of a peak at 4110 cm^{-1} in the near-infrared MCD spectrum² to the intraconfigurational $\text{E}''_g \rightarrow \text{U}'_g$ transition. We may further remark that the calculated E''_g and U'_g terms obey very precisely the $-\zeta/+(\zeta/2)$ splitting pattern, probably due to the fact that 96% of the CASSCF wave function of the ${}^2\text{T}_{2g}$ state is made up by the t_{2g}^5 configuration.

We now turn our attention to the LMCTs. The most interesting of these are of course the three ungerade LMCTs. Two different active spaces were used for the ${}^2\text{T}_{1u}$ and the ${}^2\text{T}_{2u}$ states in order to deal with the limitations on their size. For the first one, the two filled ligand shells of t_{1u} symmetry were added to AS1, obtaining the (21 in 16) active space AS2. In this active space, the three osmium 5p orbitals were kept frozen in the CASSCF calculations to prevent their entrance into the active space. SOC was calculated in the following way. In the same way, the filled ligand t_{2u} shell was added to AS1, obtaining the (15 in 13) active space AS3. The ground-state splitting was again calculated to first order in each active space. Next, in each active space, the SOC Hamiltonian was diagonalized within the available ungerade LMCT states, i.e., two (${}^2\text{T}_{1u}$ a and ${}^2\text{T}_{1u}$ b) in AS2 and one (${}^2\text{T}_{2u}$) in AS3. The results are collected in Table 2. The SOC-free transition energies were calculated with both the ECP and all-electron ANO-RCC basis sets to show that the change of basis sets has only a small influence on the results. Figure 1 shows contour plots of the CASSCF natural orbitals from which the excitations originate. As mentioned in the previous paragraph, the ground state transforms as E''_g under the double group O_h^* . The ${}^2\text{T}_{1u}$ and ${}^2\text{T}_{2u}$ terms reduce to $\text{U}'_u + \text{E}'_u$ and $\text{U}'_u + \text{E}''_u$, respectively. The fact that the LMCT states correspond to a configuration with a filled t_{2g} -d shell and one hole in a ligand shell gave rise to the idea that SOC in this terms must be negligible.² We found, however, that

(26) Griffith, J. S. *The Theory of Transition-Metal Ions*; Cambridge University Press: Cambridge, U.K., 1964.

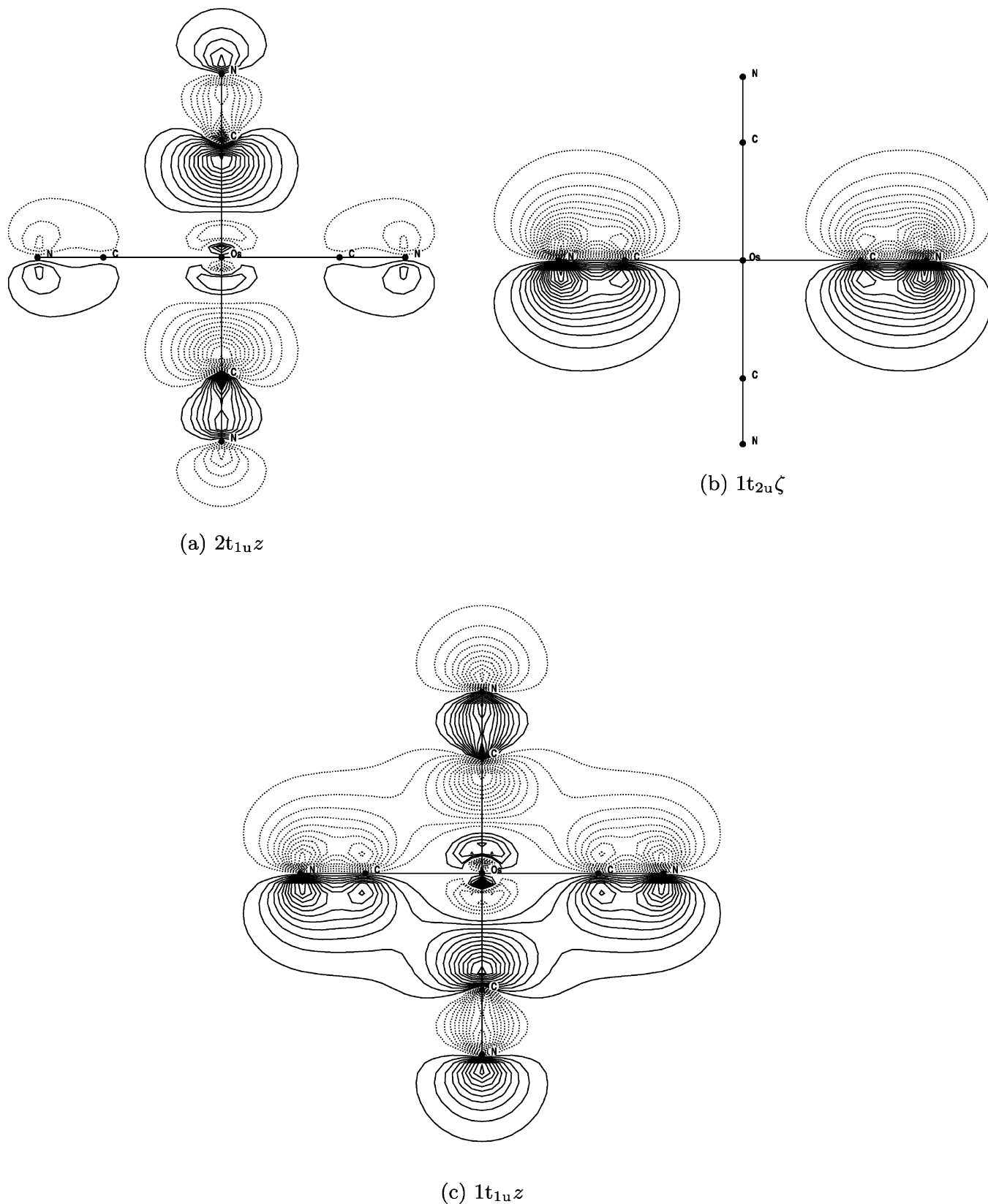


Figure 1. Contour plots of one component of the three ungerade ligand type shells. The component shown is the one representing the hole in each CASSCF LMCT state (calculated with the ECP basis set).

this is not always true. For the ${}^2T_{1u}$ a and ${}^2T_{2u}$ b terms, SOC splittings of about 2300 and 1500 cm^{-1} , respectively, were found, both attributed to the contribution of Os p character to the ligand t_{1u} orbitals. As expected for a p^5 configuration,

the U'_u term (corresponding to ${}^2P_{3/2}$) is found to be lowest in energy. In the ${}^2T_{2u}$ term, on the other hand, no Os p mixing is possible and consequently the SOC splitting appeared to be only 29 cm^{-1} .

Table 3. MLCT Excitation Energies ΔE of $[\text{Os}(\text{CN})_6]^{3-}$ Calculated with AS4 and without SOC. Excitations Are of the $t_{2g} \rightarrow t_{1u}$ Type

state D_{2h}	state O_h	main configuration	CASPT2 ^a ($\Delta E/\text{cm}^{-1}$)
${}^2\text{B}_{1g}$	${}^2\text{T}_{2g}$	t_{2g}^5	0
${}^4\text{B}_{1u}$	${}^4\text{T}_{1u}$	$t_{2g}^4 t_{1u}^1$	54 112
${}^4\text{B}_{1u}$	${}^4\text{T}_{2u}$	$t_{2g}^4 t_{1u}^1$	54 514
${}^4\text{A}_{1u}$	${}^4\text{E}_u$	$t_{2g}^4 t_{1u}^1$	54 387
${}^4\text{A}_{1u}$	${}^4\text{A}_{1u}$	$t_{2g}^4 t_{1u}^1$	54 957
${}^2\text{B}_{1u}$	${}^2\text{T}_{1u} \text{ a}$	$t_{2g}^4 t_{1u}^1$	53 452
${}^2\text{B}_{1u}$	${}^2\text{T}_{2u} \text{ a}$	$t_{2g}^4 t_{1u}^1$	53 648
${}^2\text{B}_{1u}$	${}^2\text{T}_{1u} \text{ b}$	$t_{2g}^4 t_{1u}^1$	60 346
${}^2\text{B}_{1u}$	${}^2\text{T}_{2u} \text{ b}$	$t_{2g}^4 t_{1u}^1$	61 131
${}^2\text{B}_{1u}$	${}^2\text{T}_{2u} \text{ c}$	$t_{2g}^4 t_{1u}^1$	61 931
${}^2\text{B}_{1u}$	${}^2\text{T}_{1u} \text{ c}$	$t_{2g}^4 t_{1u}^1$	62 292
${}^2\text{B}_{1u}$	${}^2\text{T}_{1u} \text{ d}$	$t_{2g}^4 t_{1u}^1$	69 797
${}^2\text{A}_u$	${}^2\text{E}_u \text{ a}$	$t_{2g}^4 t_{1u}^1$	55 456
${}^2\text{A}_u$	${}^2\text{A}_{1u}$	$t_{2g}^4 t_{1u}^1$	55 729
${}^2\text{A}_u$	${}^2\text{E}_u \text{ b}$	$t_{2g}^4 t_{1u}^1$	63 306
${}^2\text{A}_u$	${}^2\text{A}_{2u}$	$t_{2g}^4 t_{1u}^1$	63 331

^a Multistate CASPT2 for the ${}^2\text{A}_u$ and ${}^4\text{A}_u$ states of D_{2h} resulted in unwanted mixing between states of different O_h symmetry and was for that reason not used in these cases.

We shall now compare the calculated transition energies with the experimentally determined ones.² The following selection rules apply to electric-dipole transitions: $E''_g \rightarrow E''_u$, U'_u are allowed and $E''_g \rightarrow E'_u$ is forbidden. The first absorption band in the spectrum is roughly composed of one intense peak at $24\,200\text{ cm}^{-1}$ and one weak absorption at $27\,000\text{ cm}^{-1}$. The band shows some fine structure of which the origin is not clear. The whole band was assigned to the $E''_g ({}^2\text{T}_{2g}) \rightarrow {}^2\text{T}_{1u} \text{ a}$ transition.² The authors did, however, not take into consideration the SOC splitting in the LMCT state. On the basis of the calculated values and the fact that the transition to E'_u is symmetry forbidden, the intense absorption at $24\,200\text{ cm}^{-1}$ may be assigned to the $E''_g \rightarrow U'_u$ transition, calculated at $24\,861\text{ cm}^{-1}$ whereas the weak absorption at $27\,000\text{ cm}^{-1}$ may be connected with the symmetry forbidden $E''_g \rightarrow E'_u ({}^2\text{T}_{1u} \text{ a})$ transition, calculated at $27\,145\text{ cm}^{-1}$. Other possible symmetry-forbidden transitions arise from the gerade LMCT states. We calculated some of these and found that the lowest one appeared at about $37\,000\text{ cm}^{-1}$, which is too high to account for the absorption in question. The central absorption band is formed by two intense peaks at $30\,000$ and $32\,100\text{ cm}^{-1}$, assigned as vibrational components (CN^- stretching) of the $E''_g ({}^2\text{T}_{2g}) \rightarrow {}^2\text{T}_{2u}$ transition.² No SOC splitting is observed, in accordance with our calculations. The presence of this vibrational progression in the ${}^2\text{T}_{2u}$ transition can be rationalized by considering the corresponding t_{2u} orbital in Figure 1: This orbital is totally composed of the bonding $\text{CN}^- \pi$ orbitals. An excitation from this orbital to the metal reduces the electron density between the carbon and nitrogen atoms,

inducing the possibility of a vibrational excitation. On the other hand, the $2t_{1u}$ orbital is mainly composed of the $\text{CN}^- \sigma$ lone pair. An excitation from this orbital (i.e., to the ${}^2\text{T}_{1u}$ a state) is therefore not expected to cause a progression in the CN^- stretching. These considerations further support the considered assignment. The difference between the experimental location of the ${}^2\text{T}_{2u}$ peaks and the computational value of $39\,952\text{ cm}^{-1}$ is quite large in comparison with that of the ${}^2\text{T}_{1u}$ a transition. This discrepancy could be partly due to the apparent importance of vibrational progression in this state, while the calculation method does not incorporate vibrational effects. The third band of the spectrum is located at $34\,400\text{ cm}^{-1}$ and assigned as the $E''_g ({}^2\text{T}_{2g}) \rightarrow {}^2\text{T}_{1u} \text{ b}$ transition.² Again, taking into account the SOC splitting, this may better be assigned as the $E''_g \rightarrow U'_u$ transition, calculated at $40\,639\text{ cm}^{-1}$. The differences between the calculated and the experimental energies thus range from about 600 to 8000 cm^{-1} . Possible explanations are the limitations on the size of the active space, which necessarily has to be bigger than that used for ligand field calculations, where the errors on the calculated transition energies are known to be about 2000 cm^{-1} .^{6,8–11} Furthermore, the present calculations do not take into account the effect of the environment, which may have an influence on the charge-transfer energies. Although extended calculations including such effects may improve the correspondence between theory and experiment, they will not influence the assignment of the LMCT transitions, which is our present interest.

For completeness we must also consider the ungerade MLCTs to ensure that these cannot be responsible for the observed absorptions. For this purpose, the AS1 was extended with the lowest unoccupied ligand shell of ungerade symmetry, which is a t_{1u} shell (originating from the π^* LUMO orbitals of CN^-), obtaining a (9 in 13) active space: AS4. The energies of the $t_{2g}^4 t_{1u}^1$ states were calculated without SOC and are collected in Table 3. Because of the high density of states, state-averaged CASSCF was used to calculate all states belonging to the same D_{2h} irreducible representation, followed by multistate CASPT2. Since the lowest excitation occurs only at $53\,452\text{ cm}^{-1}$ it is clear that no MLCT transition can occur in the recorded spectrum, even when SOC is taken into account.

4. Conclusions

CASPT2 calculations on $[\text{Os}(\text{CN})_6]^{3-}$ have shown that the octahedral ligand field splitting parameter Δ_o is about $55\,000\text{ cm}^{-1}$. This is in accordance with the well-known increasing value of Δ_o when moving down a transition-metal group and contradicts previous experiment-based values of only $38\,000\text{ cm}^{-1}$. This high value of Δ_o prevents ligand field transitions from occurring in the experimental UV–vis spectrum. Instead, the calculations point out that the three ungerade LMCTs are the only candidates to account for the strong absorption bands in the spectrum. This finding supports the assignment of the MCD spectrum and the conclusion that some of the additional peaks (especially in the ${}^2\text{T}_{2u}$ band)

result from cyanide vibrational progression. The splitting of the ${}^2T_{2g}$ ground state due to spin-orbit coupling was found to be in agreement with the experimental value of ref 2. SOC splitting in the ${}^2T_{1u}$ LMCT states is not negligible as previously thought and may range up to 2300 cm^{-1} .

Acknowledgment. Financial support from the Flemish Science Foundation (FWO) and the Flemish Government under the Concerted Action Scheme are gratefully acknowledged.

IC7004612